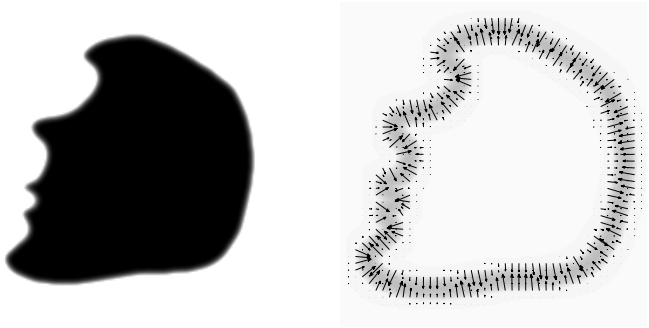

figure 3.1. *Geometric interpretation of the new term in the proposed deformable model. The gradient vectors are all directed towards the middle of the boundary. Those vectors direct the propagating curve into the valley of the g function.*

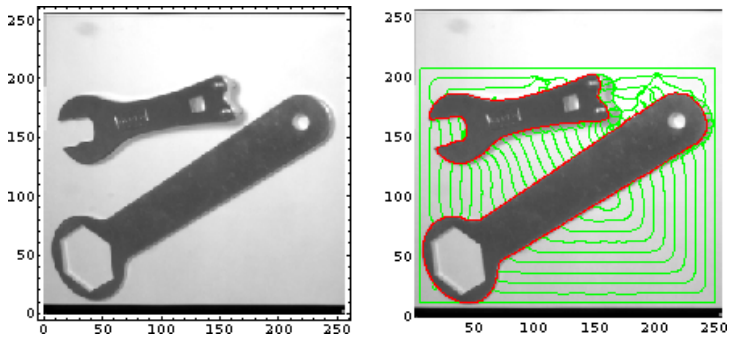

figure 3.2. *Detecting two wrenches with the geodesic flow, moving inwards.*

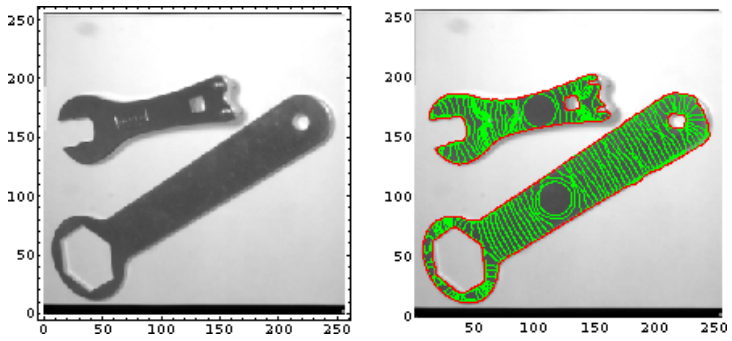

figure 3.3. *Detecting two wrenches with the geodesic flow, moving outwards.*

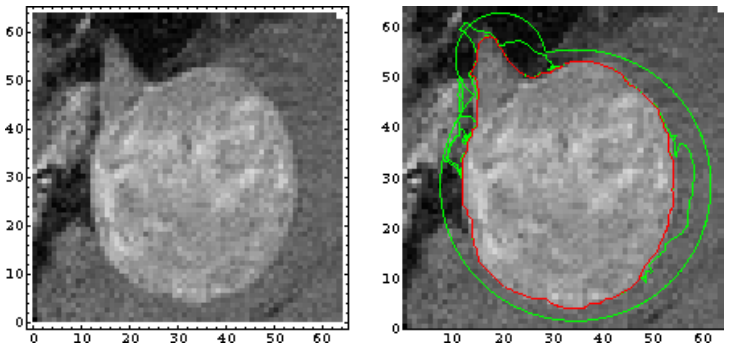

figure 3.4. *Inward geodesic flow for tumor detection.*

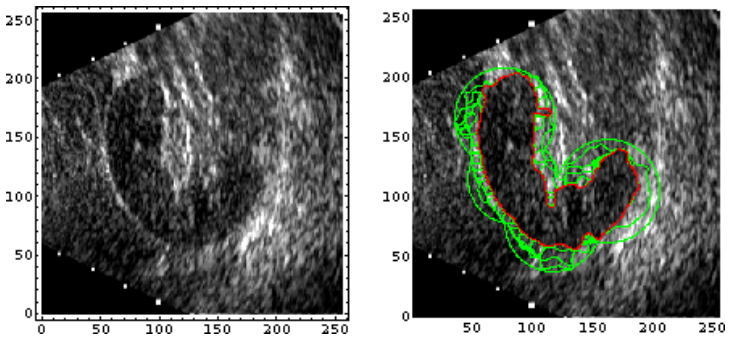

figure 3.5. *Inward geodesic flow for ultrasound detection.*

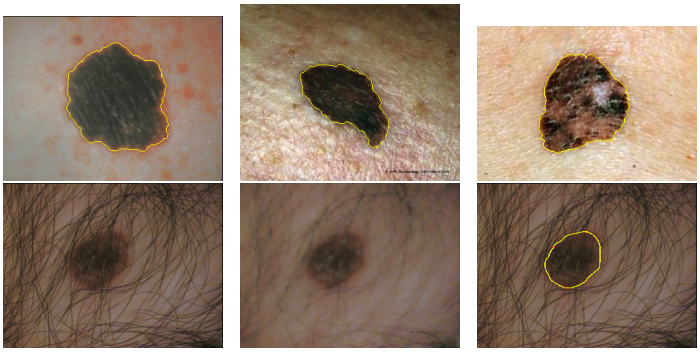

figure 3.6. *Geodesic flow for skin lesion segmentation. Three examples are given in the first row, while the second row shows the original hairy image, result of hair removal via continuous scale morphological PDE's, and the segmented lesion.*

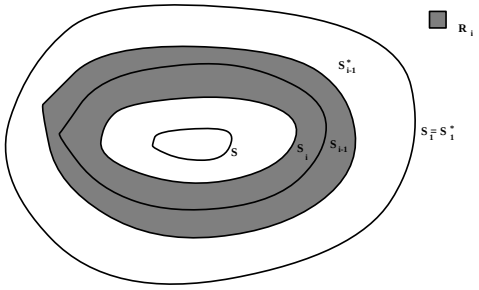

figure 3.7. *Construction for the lemma.*

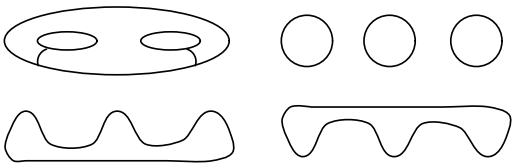

figure 3.8. *Construction of* Γ_1 *and* Γ_2.

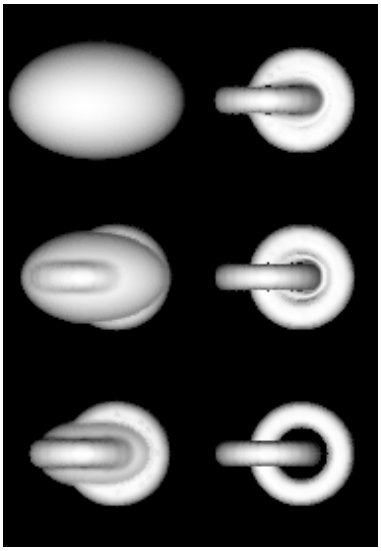

figure 3.9. *Detection of two linked tori.*

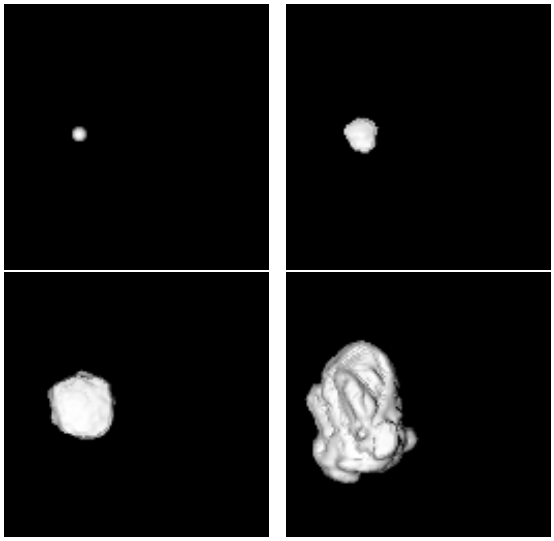

figure 3.10. *Surface evolution toward the detection of a tumor in MRI.*

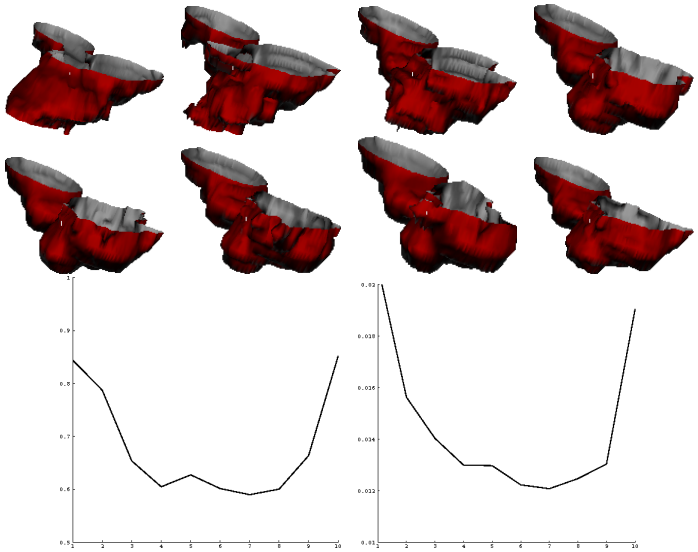

figure 3.11. *Detection of a heart with the minimal surfaces model. Several consecutive time stages are shown, together with the plot of the area and volume (vertical exes) against time (horizontal axes).*

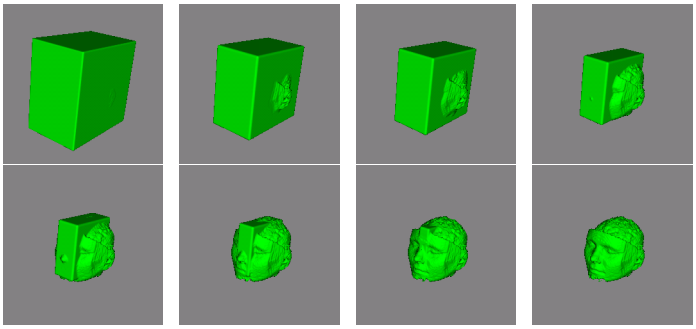

figure 3.12. *Detecting a head from 3D MRI. Eight steps of the evolution of the minimal surface are shown.*

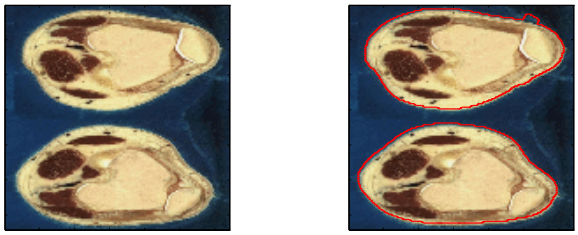

figure 3.13. *Example of the color snakes. The original image is on the left, and the one with the segmented objects (red lines) on the right. The original curve contained both objects. The computations were done on the $L^*a^*b^*$ space.*

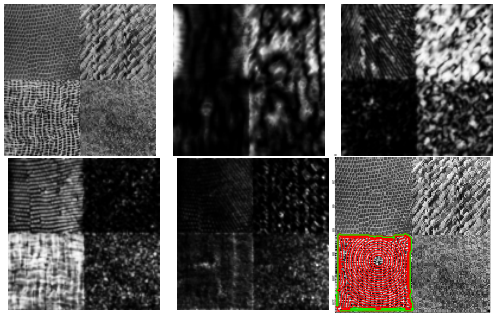

figure 3.14. *Example of the vector snakes for a texture image. The original texture (top-left) is decomposed into frequency/orientation (four frequencies and four orientations) components via Gabor filters and this collection of images is used to compute the metric g_{color} for the snakes flow. A subset of the different components are shown, followed (bottom-right) by the result of the evolving vector snakes (green), segmenting one of the texture boundaries (red).*

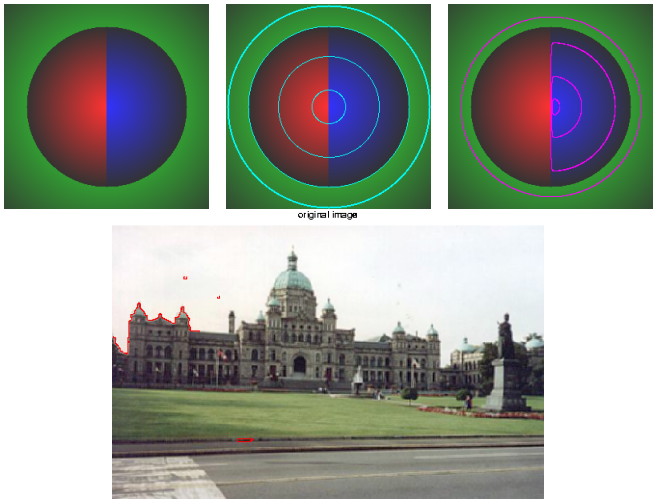

figure 3.15. *Level-sets for multivalued images. The first row shows an toy example, with original image on the left, followed by the level-lines for the corresponding gray-valued image and the level-lines for the vector-valued image. The second row shows a segment of the level-lines for the vector-valued image.*

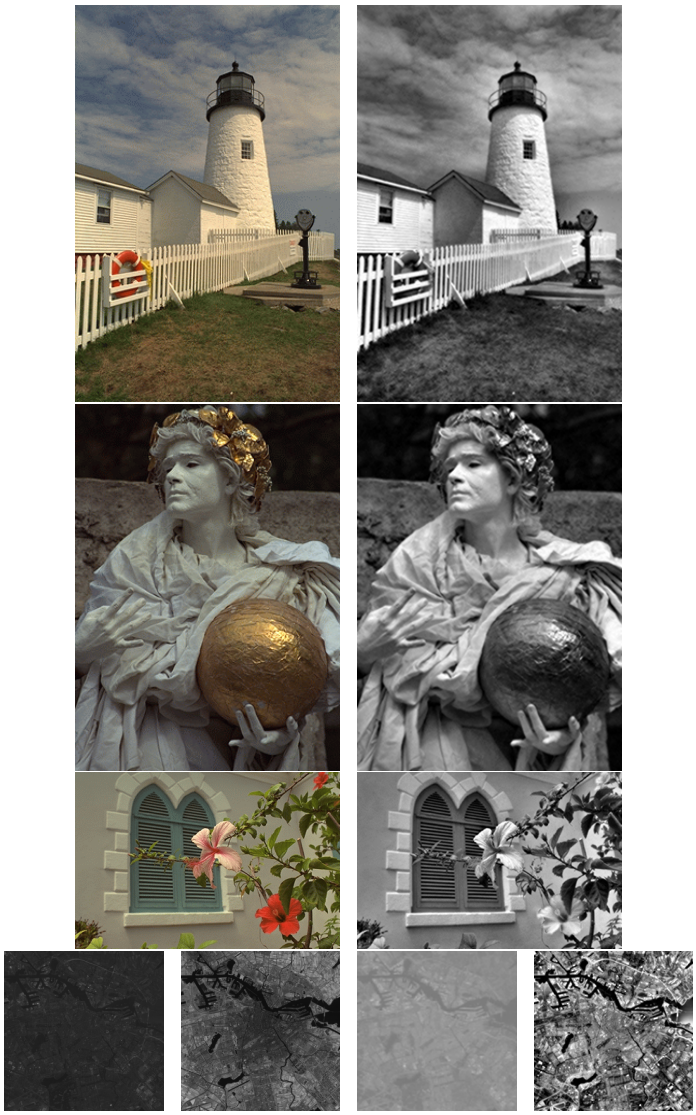

figure 3.16. *Single-valued representatives of vector-valued images. The first three rows show example for color images (vector data on the left and scalar data on the right), while the last row shows several components of LANDSAT data followed by their scalar representation.*

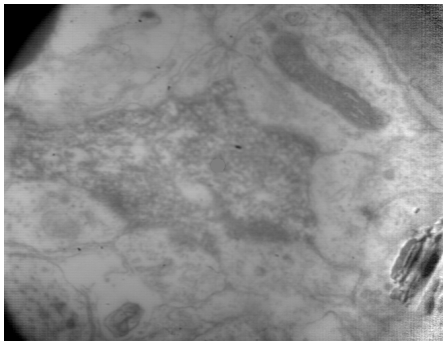

figure 3.17. *Example of an EM image of a neuron (one slice).*

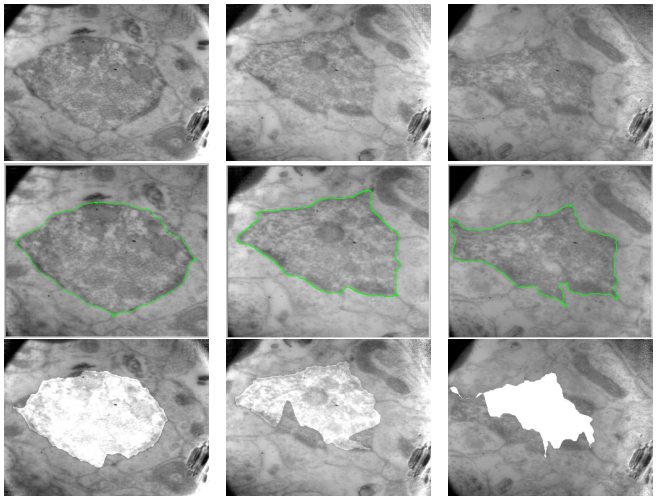

figure 3.18. *Comparison of the minimal geodesic results with those obtained with the commercial software PictureIt. For each column, the original image is shown on the top, the result of the tracing algorithm (green line) on the middle, and the result of PictureIt on the bottom. For this last, the area segmented by the algorithm is shown brighter.*

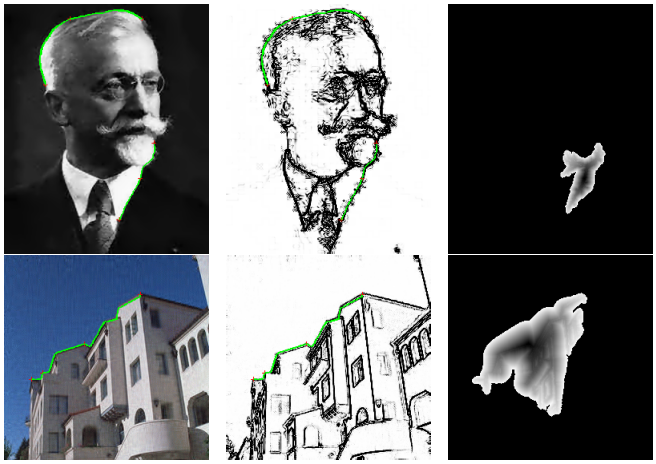

figure 3.19. *Boundary tracing with global minimal geodesics.*

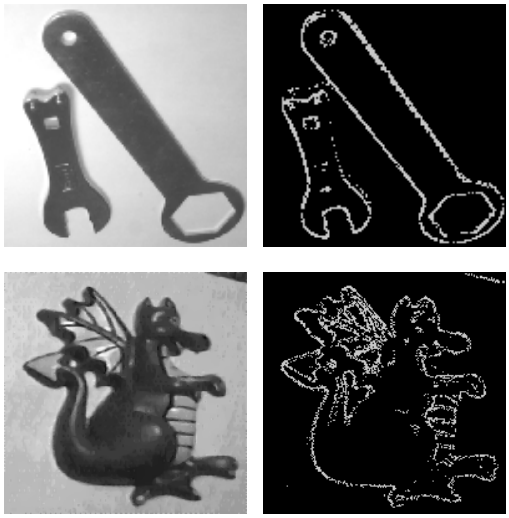

figure 3.20. *Examples of the affine invariant edge detector (after thresholding).*

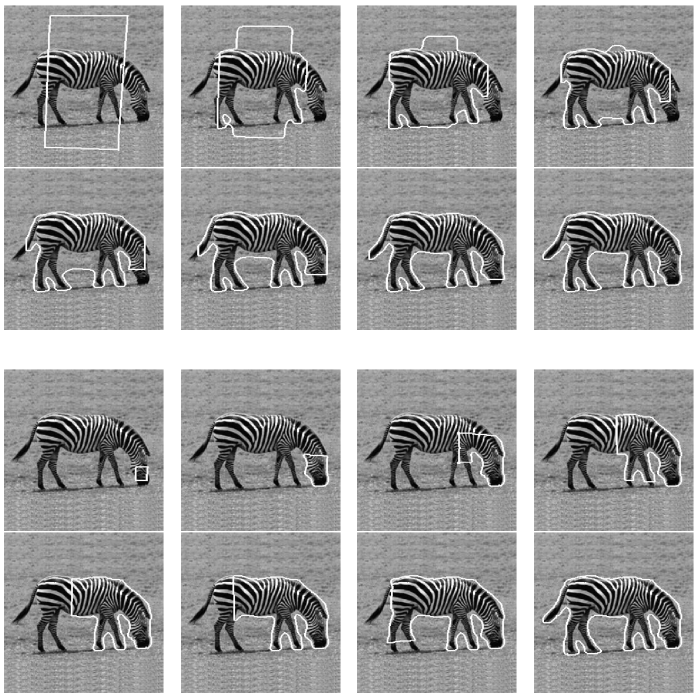

figure 3.21. *Region active contours example. The evolution of the contour is presented, for two different initial conditions. Note how for the geodesic active regions there is no need to have the initial contour completely inside or completely outside of the object of interest.*

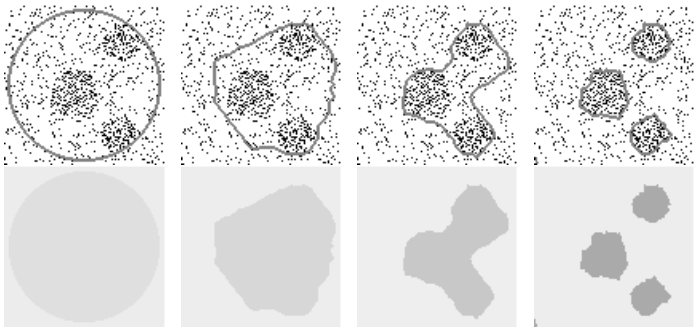

figure 3.22. *Examples of segmentation without edges. Top: Evolving curve. Bottom: Average of the approximation function inside and outside of the evolving curve.*

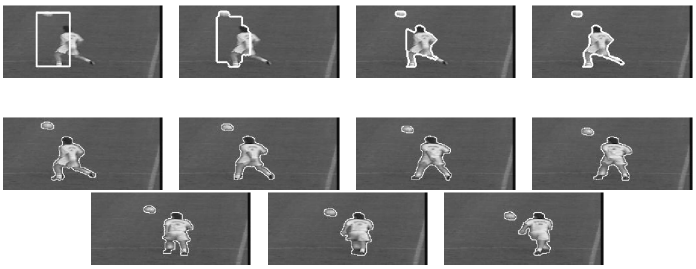

figure 3.23. *The first row shows the detection of moving objects, using both spatial and temporal "gradients." The second and third rows show the tracking with the active regions scheme by Paragios and Deriche. The algorithm combines optical flow computation and moving object detection.*

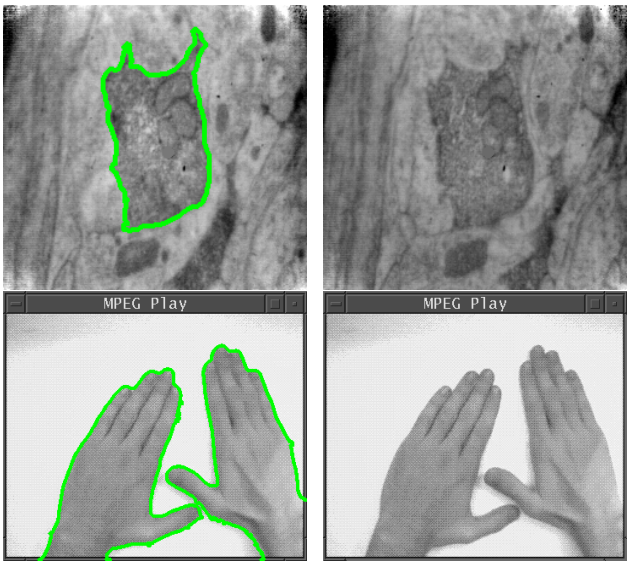

figure 3.24. *Examples of the problems addressed in this section. See text.*

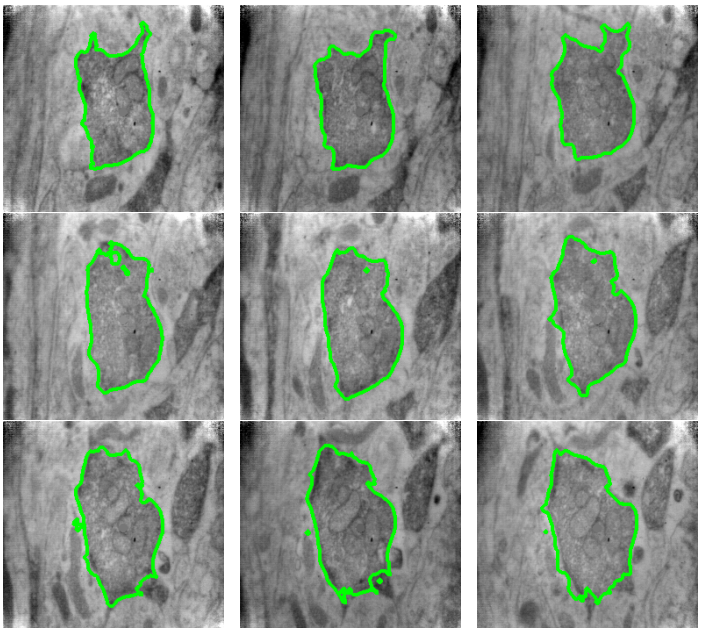

figure 3.25. *Nine consecutive slices of neural tissue. The first image has been segmented manually. The segmentation over the sequence has been performed using the algorithm described in this section.*

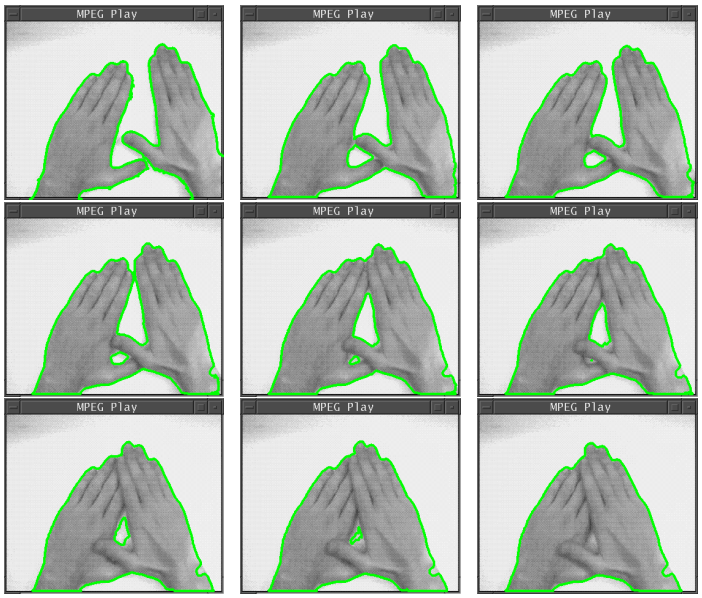

figure 3.26. *Nine frames of a movie. The first image has been segmented manually. The segmentation over the sequence has been performed using the algorithm described in this section. Notice the automatic handling of topology changes.*

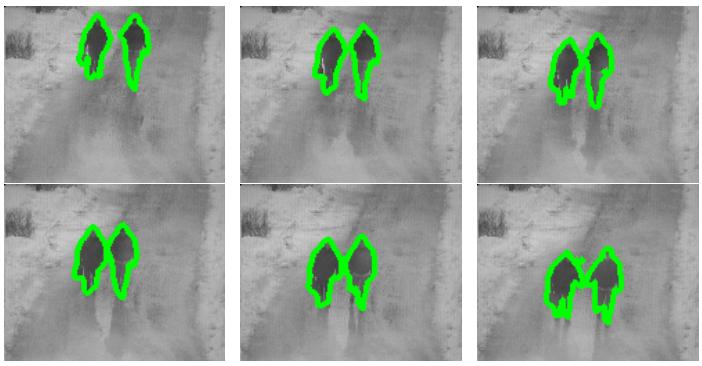

figure 3.27. *Tracking example on the "Walking swedes" movie (data courtesy of Dr. Nikos Paragios and Prof. Rachid Deriche).*

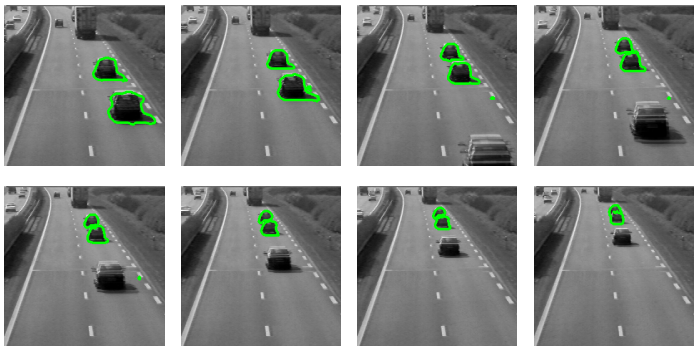

figure 3.28. *Tracking example on the "Highway" movie (data courtesy of Dr. Nikos Paragios and Prof. Rachid Deriche).*

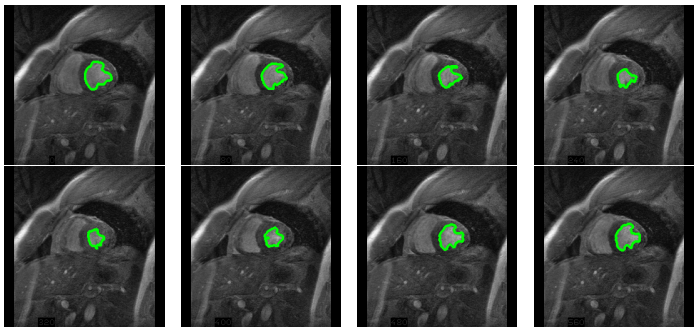

figure 3.29. *Tracking example on the "Heart" movie (data courtesy of Prof. Allen Tannenbaum).*

figure 3.30. *3D reconstruction from a stereo pair using the geodesic stereo approach. First, the stereo pair is shown, followed by the reconstructed 3D shape.*